Published in final edited form as:

J Nat Prod. 2010 March 26; 73(3): 383–387. doi:10.1021/np900281r.

Anti-infective Discorhabdins from a Deep-Water Alaskan Sponge of the Genus *Latrunculia*†

MinKyun Na[‡,§], **Yuanqing Ding**[‡], **Bin Wang**[‡], **Babu L. Tekwani**[‡], **Raymond F. Schinazi**[⊥], **Scott Franzblau**[‖], **Michelle Kelly**[▽], **Robert Stone**[○], **Xing-Cong Li**[‡], **Daneel Ferreira**[‡], and **Mark T. Hamann**[*,‡]

[‡]Department of Pharmacognosy and the National Center for Natural Products Research (NCNPR), School of Pharmacy, The University of Mississippi, University, Mississippi 38677 [§]College of Pharmacy, Yeungnam University, Gyeongsan, Gyeongbuk 712-749, South Korea [⊥]Department of Pediatrics, Emory University/VA Medical Center, Decatur, Georgia 30033 [‖]Institute for Tuberculosis Research, College of Pharmacy, University of Illinois at Chicago, Chicago, Illinois 60607 [▽]National Centre for Aquatic Biodiversity and Biosecurity, National Institute of Water and Atmospheric Research (NIWA), Private Bag 109695, Auckland, New Zealand [○]Auke Bay Laboratories, Alaska Fisheries Science Center, NOAA Fisheries, 17109 Point Lena Loop Road Juneau, Alaska 99801

Abstract

Bioassay- and LC-MS-guided fractionation of a methanol extract from a new deep-water Alaskan sponge species of the genus *Latrunculia* resulted in the isolation of two new brominated pyrroloiminoquinones, dihydrodiscorhabdin B (**1**) and discorhabdin Y (**2**), along with six known pyrroloiminoquinone alkaloids, discorhabdins A (**3**), C (**4**), E (**5**), and L (**6**), dihydrodiscorhabdin C (**7**), and the benzene derivative **8**. Compounds **3**, **4**, and **7** exhibited anti-HCV activity, antimalarial activity, and selective antimicrobial activity. Although compounds **3** and **7** displayed potent and selective *in vitro* antiprotozoal activity, *Plasmodium berghei*-infected mice did not respond to these metabolites due to their toxicity *in vivo*.

The genus *Latrunculia* (class Demospongiae, order Poecilosclerida, family Latrunculiidae) is predominantly found in cold water regions such as Antarctica and the North Pacific, particularly in South Africa and New Zealand.[1] *Latrunculia* species are commonly reported down to −30 m[1] and usually lead to the discovery of many types of constituents including the cytotoxic discorhabdin class of pyrroloiminoquinone alkaloids.[2] When evaluating extracts of invertebrates collected from Alaska by NOAA during deep-ocean trawls (−230 m), a new deep-water sponge species of the genus *Latrunculia* was found to have significant

†Dedicated to the late Dr. John W. Daly of NIDDK, NIH, Bethesda, Maryland, and to the late Dr. Richard E. Moore of the University of Hawaii at Manoa for their pioneering work on bioactive natural products.

*To whom correspondence should be addressed. Tel: +1-662-915-5730. Fax: +1-662-915-6975. ; Email: mthamann@olemiss.edu.

Supporting Information Available: NMR spectra and LC-MS data for compounds **1**–**8**; experimental CD data of discorhabdin A (**3**); and thermodynamic parameters (TPs), frequencies (Frs), and optimized *Z*-matrixes of discorhabdin Y (**2**) are available free of charge via the Internet at http://pubs.acs.org.

antiviral activity against hepatitis virus C (HCV), antimalarial activity against *Plasmodium falciparum*, and antimicrobial effects against the AIDS opportunistic pathogens methicillin-resistant *Staphylococcus aureus* (MRSA), *Mycobacterium intracellulare*, and *M. tuberculosis*. By means of bioassay- and LC-MS-guided fractionation, we isolated a group of pyrroloiminoquinone alkaloids, including two new compounds (**1** and **2**), as the active principles. In this paper, we describe the isolation, structure elucidation of the alkaloids, and the evaluation of their anti-infective properties. *In vivo* antimalarial activity using *P. berghei*-infected mice is presented for the two most active metabolites.

Results and Discussion

Analysis of the active fractions by LC-MS revealed characteristic ion clusters of mono- and dibrominated metabolites, and their ^{1}H NMR data in DMSO-d_6 showed characteristic pyrroloiminoquinone resonances [δ_H 2.8–4.0 (H-16 and H-17), 7.1–7.7 (H-1, H-4, H-5, and H-14), 7.8–8.5 (NH-18), 9.5–10.5 (NH-9), and 13.0–14.0 (NH-13)]. Further fractionation led to the isolation of a series of pyrroloiminoquinone alkaloids, including the new compounds dihydrodiscorhabdin B (**1**) and discorhabdin Y (**2**), as well as the known discorhabdins A (**3**),[3] C (**4**),[3,4] E (**5**),[5] and L (**6**),[6] dihydrodiscorhabdin C (**7**),[5] and the benzene derivative **8**.[5] It is possible that **8** is artificially produced by a dienol–benzene rearrangement from dihydrodiscorhabdin C during the isolation process.[5] The structures of the known compounds were determined by MS and NMR data and confirmed by comparing the physical and spectroscopic data with those in the literature.

Compound **1** was obtained as a dark green solid. The LRESIMS spectrum of **1** showed an ion cluster at m/z 416 and 418 $[M + H]^+$ in a 1:1 ratio, which indicated the presence of one bromine atom. The molecular formula $C_{18}H_{14}BrN_3O_2S$, the same as that found for discorhabdin A (**3**),[3] was determined by the quasi-molecular ion peak at m/z 416.0267 $[M + H]^+$ obtained by HRESIMS. The UV spectrum displayed characteristic absorptions at 405, 360, and 250 nm for a cross-conjugated pyrrolo[1,7]phenanthroline chromophore.[3-6] The ^{1}H NMR (MeOH-d_4) spectrum of **1** showed the characteristic signals for a pyrroloiminoquinone at δ_H 2.26 (1H, dd, J = 11.2, 3.2 Hz, H-7b), 2.54 (1H, d, J = 11.2 Hz, H-7a), 2.88 (2H, m, H-16), 3.71 (1H, m, H-17b), and 3.90 (1H, m, H-17a). Similarly to discorhabdins A (**3**) and B,[3] the observation of a doublet at δ_H 5.32 (1H, d, J = 3.2 Hz) implied the presence of a thioester bridge between C-5 and C-8, which was supported by the characteristic ^{13}C chemical shifts of the thiomethine carbon at δ_H 60.8 (C-8) and a quaternary carbon at δ_H 149.4 (C-5). The significant differences in the ^{1}H NMR data of **1** as compared to discorhabdin B were the presence of an oxymethine (δ_H 4.73, 1H, d, J = 6.0 Hz) coupled with the olefinic H-4 signal (δ_H 5.61, 1H, d, J = 6.0 Hz) and the upfield chemical shift (Δ 1.3 ppm) of the H-1 signal (δ_H 6.66, 1H, s). This suggested that the ketone in the 1,4-cyclohexadiene ring is changed to an alcohol at C-3, which was further supported by the oxymethine signal (δ_C 69.8) appearing in the 13C NMR (MeOH-d_4) spectrum. In addition, the 1,4-cyclohexadiene structure of **1** was confirmed by HMBC correlations from the hydroxy methine proton to C-1 (δ_C 134.4), C-2 (δ_C 128.2), C-4 (δ_C 115.8), and C-5 (δ_C 149.4) (Figure 1). The NOESY NMR (MeOH-d_4) data, which showed correlations from H-8 (δ_H 5.42, d, J = 3.2 Hz) to both the H-7 protons (δ_H 2.54, d, J = 11.2 Hz and 2.26, dd, J =

11.2, 3.2 Hz) and from H-1 (δ_H 6.66, s) to H-7a (δ_H 2.54, d, J = 11.2 Hz) supported that **1** had the same relative configuration as those of discorhabdins A and B.[3] When collecting optical rotation and CD data for **1**, the compound decomposed, and we currently lack access to more sponge material, so the absolute configuration of **1** is not assigned. To follow the naming system of the discorhabdins,[2,7] the new compound **1** was named dihydrodiscorhabdin B.

Compound **2** was obtained as a purple solid, and its UV data were similar to those of the discorhabdins. The LRESIMS spectrum of **2** displayed quasi-molecular ions at m/z 386 and 388 $[M + H]^+$, the isotope pattern being indicative of the presence of one bromine atom. A difference of two mass units compared to discorhabdin E ($C_{18}H_{15}BrN_3O_2$)[5] indicated that one of the double bonds is saturated. The ^{1}H NMR (MeOH-d_4) spectrum of **2** revealed 12 protons in the aliphatic region and two olefinic protons, supporting the notion that one of double bonds, likely in the 1,4-cyclohexadienone ring of discorhabdin E, is saturated. Analysis of COSY (MeOH-d_4) data (see Supporting Information) established the connectivity between H-4 (δ_H 2.87, dd, J = 14.8, 5.2 Hz and 3.16, multiplicity is unclear due to signal overlap) and H-5 (δ_H 2.47, t, J = 14.8 Hz and 2.20, dd, J = 14.8, 3.6 Hz), between H-7 (δ_H 1.80, dt, J = 13.6, 4.8 Hz and 2.33, br d, J = 13.6 Hz) and H-8 (δ_H 3.69, ddd, J = 16.0, 4.8, 2.8 Hz and 3.55, ddd, J = 16.0, 13.6, 2.8 Hz), and between H-16 (δ_H 2.92, t, J = 7.6 Hz) and H-17 (δ_H 3.85, m and 3.80, m). The absolute configuration of **2** was assigned as 6*R* by comparison of the experimental CD spectrum with simulated electronic circular dichroism (ECD) spectra calculated by time-dependent density functional theory (TDDFT).[8] The theoretically calculated ECD spectrum of the formate of 6*R*-**2** agrees with the observed CD data (Figure 2). Molecular orbital (MO) analysis has been carried out at the B3LYP/6-31G** level in the gas phase, indicating that the experimentally negative Cotton effects (CEs) near 400 and 266 nm correspond to n→π* (388 nm, MO92→MO99) and π→π* (272 nm, MO96→MO100) electronic transitions (Figure 3, Table 1), and those at 291 and 218 nm are contributed by the electronic transfers (299 nm, MO98→MO100 and 204 nm, MO97→MO102). The positive CE in the experimental ECD at 360 nm results from the π→π* electronic transition (377 nm, MO95→MO99) and the electronic transfer (371 nm, MO94→MO99). The experimental high-amplitude positive CE at 244 nm may be overlapped by a series of electronic transitions in the 208–270 nm region, and the predominant one near 230 nm results from a σ→π* electronic transfer (MO88→MO99). Discorhabdins E[5] and G[9] have C-4–C-5 and C-7–C-8 double bonds, respectively. Thus, compound **2**, with both of these olefinic bonds being saturated, is a new compound that may be named either 4,5-dihydrodiscorhabdin E or 7,8-dihydrodiscorhabdin G. In order to prevent confusion, we prefer to name the new analogue discorhabdin Y.

Owing to the unique structures of the discorhabdins and their potent cytotoxicity, pyrroloiminoquinones have attracted attention as a promising lead structure for the development of possible anticancer agents.[2] Most studies of these metabolites have focused on their cytotoxicity, and no reports of antimalarial activity have been published. On the basis of the preliminary screening, we explored the antiviral, antimalarial, and antimicrobial activities in selected *in vitro* assay systems. The major constituents **3**, **4**, and **7** were evaluated for their *in vitro* antiviral activity in the HCV Huh-7 replicon assay, and the results

are presented in Table 2. Although the compounds displayed anti-HCV activity with EC_{90} values less than 10 μM, they were also cytotoxic toward Huh-7 clone B cells. The *in vitro* antimalarial activity of the major pyrroloiminoquinones was assayed against both the D6 (chloroquine-susceptible) and W2 (chloroquine-resistant) clones of *P. falciparum*, and their toxicity was evaluated against a nontransformed mammalian cell line, namely, monkey kidney fibroblasts (Vero) (Table 2). The index of selectivity (SI = $IC_{50\ Vero}/IC_{50\ P.\ falciparum}$) indicates the specificity of compounds against the parasite. Compounds **3**, **4**, and **7** showed antiprotozoal activity against the D6 clone, with IC_{50} values of 53, 2800, and 170 nM, respectively, as well as the W2 clone, with IC_{50} values of 53, 2000, and 130 nM, respectively. In addition, the major pyrroloiminoquinones exhibited selective antimicrobial activity against the AIDS opportunistic pathogens MRSA, *M. intracellulare*, and *M. tuberculosis* (Table 3). Because **3** and **7** showed potent and selective *in vitro* antimalarial activity, their *in vivo* antimalarial activity was investigated in a *Plasmodium berghei* mouse malaria model. Two groups of mice (five in each group) infected with *P. berghei* were treated with 10 mg/kg of **3** and **7** on day 0 (2 h after the infection), and the control group was administered an equal amount of SSV (the vehicle). No apparent toxicity was observed in animals treated with both compounds on day 0. However, on day 1, all the animals treated with **7** showed signs of toxicity such as loss of weight, reduction of movements, and dehydration. One of the mice died on day 3 and the others on day 4 before examination for parasitemia. Animals treated with **3** did not show any external symptoms on day 1 and received the second dose of compound (10 mg/kg). However, animals in this group also exhibited signs of toxicity from day 2 and one of them died on day 4. Blood smears were prepared from the remaining four mice on day 5. Although around 50% suppression of parasitemia was observed in this group (Table 4), the mice were euthanized due to the significant loss of weight (>25%) and severe signs of toxicity.

Experimental Section

General Experimental Procedures

Optical rotations were measured on a JASCO DIP-370 polarimeter. CD spectra were obtained on a JASCO J-715 spectropolarimeter. UV–vis spectra were recorded on an Agilent 1100 series diode array and multiple wavelength detectors (DAD). The LC-MS analyses were performed with an Agilent 1100 HPLC system applying a Phenomenex Luna 5 μm $C_8(2)$ column (4.6 mm × 150 mm), MeCN–H_2O (0.1% HCOOH) gradient solvent system, and a Bruker Daltonics microTOF mass spectrometer. HRESIMS spectra were measured using the LC-MS system with electrospray ionization. NMR spectra were obtained on Bruker Avance DRX-400 MHz and Varian Unity Inova 400 MHz spectrometers using methanol-d_4 or DMSO-d_6 (Aldrich) as solvents. Column chromatography was conducted using silica gel 60 (40–63 μm particle size) and RP-18 (40–63 μm particle size). Precoated TLC silica gel 60 F_{254} plates from Merck were used for TLC. HPLC was carried out using a Waters System equipped with a Waters model 2487 dual λ absorbance detector and Phenomenex C_8 and C_{18} columns (21.2 × 250 mm or 10 × 250 mm, 5 μm particle size) for preparative runs.

Sponge Material

The sample was collected by dredge from the Aleutian Islands (latitude 53.06264 N, longitude −169.0872) by the Alaska Fisheries Science Center *F/V Gladiator* at a depth of −230 m on June 12, 2004 (Station 279-48, Cruise 200401, Haul 25). The sponge forms a hemispherical mound with raised areolate buttons and several apical oscules. The color of the live sponge is dark chocolate brown with deep green and purple tinges; the texture is soft and compressible. The sponge is similar to *Latrunculia (biannulata) oparinae* Samaai & Krasokhin, 2002, also from the North Pacific, with acanthose styles and short squat discorhabds, but it differs in the overall length of the megascleres and the morphology of the annual rings on the discorhabd microscleres. *L. oparinae*, in the subgenus *biannulata*, has only two annual rings on the microsclere, whereas the present sample has three annual rings and a manubrium spine, placing it within the subgenus *latrunculia*. The specimen thus represents a new and as yet undescribed species of *Latrunculia* (order Poecilosclerida, family Latrunculiidae). Voucher specimens have been deposited in the Natural History Museum, London [BMNH2006.8.24.1 (University of Mississippi voucher 04AK-018, NIWA voucher NIWAKD4823) and BMNH2006.8.24.2 (University of Mississippi voucher 04AK-018B, NIWA voucher NIWAKD4401)].

Extraction and Isolation

The frozen sponge was homogenized and extracted with EtOH at room temperature. The crude extract (50 g) was subjected to VLC on a silica gel column (15.5 × 10 cm) eluting with a stepwise gradient solvent of hexanes–EtOAc (100:0, 70:30, 50:50, 30:70, 0:100) and EtOAc–MeOH (90:10, 70:30, 50:50, 30:70, 0:100), then MeOH–H_2O (50:50, 0:100), to yield 12 fractions. The anti-HCV, antiprotozoal, and antimicrobial activities were concentrated in Fr-7 and Fr-8. Fr-7 (4.44 g) was chromatographed over silica gel (5.5 × 30 cm) using a gradient of $CHCl_3$–MeOH (from 100:0 to 0:100), followed by preparative HPLC [Phenomenex C_8 column (21.2 × 250 mm); flow rate 5 mL/min using a gradient from 20% to 80% MeOH × in H_2O (0.05% HCOOH), or 20% to 35% MeCN in H_2O (0.1% formic acid), or 32% to 100% MeCN in H_2O] to afford **1** (2.6 mg), **2** (0.3 mg), **3** (87.4 mg), **4** (112.2 mg), **5** (5.5 mg), **7** (198.5 mg), and **8** (1.0 mg). Fr-8 (4.95 g) was divided into MeOH-soluble and -insoluble fractions. A portion of the former (910 mg) was fractionated by preparative HPLC [Phenomenex C_{18} column (21.2 × 250 mm); mobile phase MeCN–H_2O (10:90) at flow rate of 5 mL/min] to afford **6** (3.9 mg).

Computational Chemistry

Density functional theory (DFT) calculations, using Gaussian 03, were employed to optimize the ground state geometries at 298 K in the gas phase at the B3LYP/6-31G** level by using default convergence. Harmonic frequencies were calculated to confirm the minimum. The geometry of the ground state was then used to calculate the ECD by using TDDFT at the B3LYP/6-31G** and B3LYP/aug-cc-pVDZ//B3LYP/6-31G** levels in the gas phase. The calculated excitation energies ΔE_i (in nm) and rotatory strength (R_i) were then simulated into ECD curves by using the Gaussian function

$$\Delta \in (E) = \frac{1}{2.297 \times 10^{-39}} \frac{1}{\sqrt{2\pi\sigma}} \sum_{i}^{A} \Delta E_i R_i e^{-[(E-\Delta E_i)/(2\sigma)]^2}$$

where σ is the width of the band at 1/e height and ΔE_i and R_i are the excitation energies and rotatory strengths for transition *i*, respectively. In the current work a value of σ = 0.20 eV and rotatory strength in the dipole length form (R_{len}) were used.

Dihydrodiscorhabdin B (1)

dark brown-green solid as the formate salt; UV (DAD) λ_{max} 250, 360, 405 nm; ^{1}H NMR (MeOH-d_4, 400 MHz) δ 8.53 (1H, br s, NH-18), 7.12 (1H, s, H-14), 6.66 (1H, s, H-1), 5.61 (1H, d, *J* = 6.0 Hz, H-4), 5.42 (1H, d, *J* = 3.0 Hz, H-8), 4.73 (1H, d, *J* = 6.0 Hz, H-3), 3.90 (1H, m, H-17a), 3.71 (1H, m, H-17b), 2.88 (2H, m, H-16), 2.54 (1H, d, *J* = 11.2 Hz, H-7a), 2.26 (1H, dd, *J* = 11.2, 3.2 Hz, H-7b); ^{13}C NMR (MeOH-d_4, 100 MHz) δ 167.2 (C-11), 156.5 (C-19), 152.7 (C-10), 149.4 (C-5), 134.4 (C-1), 128.2 (C-2), 127.5 (C-14), 125.5 (C-12), 124.6 (C-21), 121.2 (C-15), 115.8 (C-4), 100.8 (C-20), 69.8 (C-3), 60.8 (C-8), 50.9 (C-6), 45.0 (C-17), 44.8 (C-7), 19.3 (C-16); HRESIMS *m*/*z* 416.0005 $[M + H]^+$ (calcd for $C_{18}H_{15}{}^{79}BrN_3O_2S$, 416.0068) and 417.9983 $[M + H]^+$ (calcd for $C_{18}H_{15}{}^{81}BrN_3O_2S$, 418.0048).

(+)-6*R*-Discorhabdin Y (2)

purple solid as the formate salt; $[\alpha]_D^{25}$ +20 (*c* 0.01, MeOH); CD (MeOH) λ_{max} ($\Delta\varepsilon$) 218 nm (−0.57), 244 nm (1.11), 266 nm (−0.35), 360 nm (0.20); UV (DAD) λ_{max} 250, 338, 400 nm; ^{1}H NMR (MeOH-d_4, 400 MHz) δ 7.39 (1H, s, H-1), 7.17 (1H, s, H-14), 3.85 (1H, m, H-17a), 3.80 (1H, m, H-17b), 3.69 (1H, ddd, *J* = 16.0, 4.8, 2.8 Hz, H-8a), 3.55 (1H, ddd, *J* = 16.0, 13.6, 2.8 Hz, H-8b), 3.16 (signal overlapped, H-4), 2.92 (2H, t, *J* = 7.6 Hz, H-16), 2.87 (1H, dd, *J* = 14.8, 5.2 Hz, H-4), 2.47 (1H, t, *J* = 14.8 Hz, H-5a), 2.33 (1H, br d, *J* = 13.6 Hz, H-7a), 2.20 (1H, dd, *J* = 14.8, 3.6 Hz, H-5b), 1.80 (1H, dt, *J* = 13.6, 4.8 Hz, H-7b); HRESIMS *m*/*z* 386.0586 $[M + H]^+$ (calcd for $C_{18}H_{17}{}^{79}BrN_3O_2$, 386.0504) and 388.0582 $[M + H]^+$ (calcd for $C_{18}H_{17}{}^{81}BrN_3O_2$, 388.0504).

Discorhabdin A (3)

dark brown-green solid as the formate salt; CD (MeOH) λ_{max} ($\Delta\varepsilon$) 216 nm (−6.92), 250 nm (1.29), 267 nm (−1.36), 326 nm (2.91), 390 nm (−0.28); NMR and CD data consistent with those in the literature;[3] ESIMS *m*/*z* 416.0/418.0 (1:1) $[M + H]^+$.

Discorhabdin C (4)

dark purple crystal as the formate salt; $[\alpha]_D^{25}$ 0 (*c* 0.03, MeOH) (lit.[3] $[\alpha]^{25}_D$ 0); NMR data consistent with those in the literature;[3,4] ESIMS *m*/*z* 461.9/463.9/465.9 (1:2:1) $[M + H]^+$.

Dihydrodiscorhabdin C (7)

dark purple solid as the formate salt; $[\alpha]_D^{25}$ 0 (*c* 0.02, MeOH); NMR data consistent with those in the literature;[5] ESIMS *m*/*z* 464.0/466.0/468.0 (1:2:1) $[M + H]^+$.

HCV Replicon Assay[10]

Huh-7 clone B cells containing HCV replicon RNA were seeded in a 96-well plate at 5000 cells/well, and the compounds were added in duplicate at 10 μM. Following five-days incubation (37 °C, 5% CO_2), the total cellular RNA was isolated using the RNeasy 96-kit, Qiagen. Replicon RNA and an internal control (TaqMan rRNA control reagents, Applied Biosystems) were amplified in a single-step multiplex RT-PCR assay. To express the antiviral effectiveness of the compound, the threshold RT-PCR cycle of the test compound was subtracted from the average threshold RT-PCR cycle of the no-drug control (ΔCt_{HCV}). A ΔCt of 3.3 equals a 1 − log reduction (equal to the 90% effective concentration [EC_{90}]) in replicon RNA levels. The cytotoxicity of the test compounds was also expressed by calculating the ΔCt_{rRNA} values.

Antimalarial and Antimicrobial Assays

In vitro antimalarial activity was determined on chloroquine-sensitive (D6, Sierra Leone) and -resistant (W2, Indo-China) strains of *P. falciparum*.[11] *In vivo* tests were performed under the protocols of the NCNPR. Mice were infected intravenously with *P. berghei*-infected red blood cells (2×10^6) and treated subcutaneously or orally with 10 mg/kg of a solution of the test compounds at 2 h (day 0) and on day 1 post-infection. Parasitemia was determined by microscopic examination on day 5 and expressed as percentages of the mean parasitemias. *In vitro* antimicrobial activity against AIDS opportunistic pathogens and antituberculosis activity against *M. tuberculosis* were evaluated by previously published procedures.[12]

Supplementary Material

Refer to Web version on PubMed Central for supplementary material.

Acknowledgment

We thank the Mississippi Center for Supercomputing Research (MCSR) for computational facilities. Financial support for this project was provided by the NIH (NCRR P20 RR021929, C06 RR1450301, NIAID AI 27094, R-01 AI 36596-12), CDC (NCZVED U01/CI000211), and NSF (EPS-0556308). The antiprotozoal and antimicrobial assays at NCNPR are supported by the USDA-ARS Agricultural Research Service Specific Cooperative Agreement 58-6408-2-2-0009. The authors are thankful to Mr. J. Trott for performing the *in vitro* antimalarial assays and R. Sahu for *in vivo* antimalarial evaluation. R.F.S. is supported in part by a Center for AIDS research NIH grant 2P30-AI050409 and the Department of Veterans Affairs.

References and Notes

(1). (a) Lehnert H, Stone R, Heimler W. Zootaxa. 2006; 1250:1–35.(b Samaai T, Krasokhin V. Beaufortia. 2002; 52:95–101.(c) Samaai T, Gibbons MJ, Kelly M, Davies-Coleman M. Zootaxa. 2003; 371:1–26.

(2). Antunes EM, Copp BR, Davies-Coleman MT, Samaai T. Nat. Prod. Rep. 2005; 22:62–72. [PubMed: 15692617]

(3). (a) Perry NB, Blunt JW, Munro MHG. Tetrahedron. 1988; 44:1727–1734.(b) Grkovic T, Ding Y; Li X-C; Webb VL, Ferreira D, Copp BR. J. Org. Chem. 2008; 73:9133–9136. [PubMed: 18855481]

(4). Perry NB, Blunt JW, McCombs JD, Munro MHG. J. Org. Chem. 1986; 51:5478–5480.

(5). Copp BR, Fulton KF, Perry NB, Blunt JW, Munro MHG. J. Org. Chem. 1994; 59:8233–8238.

(6). Reyes F, Martín R, Rueda A, Fernández R, Montalvo D, Gómez C, Sánchez-Puelles JM. J. Nat. Prod. 2004; 67:463–465. [PubMed: 15043433]

(7). (a) Antunes EM, Beukes DR, Kelly M, Samaai T, Barrows LR, Marshall KM, Sincich C, Davies-Coleman MT. J. Nat. Prod. 2004; 67:1268–1276. [PubMed: 15332840] (b) El-Naggar M, Capon RJ. J. Nat. Prod. 2009; 72:460–464. [PubMed: 19226152]

(8). (a) Diedrich C, Grimme S. J. Phys. Chem. A. 2003; 107:2524–2539.(b) Crawford TD, Tam MC, Abrams ML. J. Phys. Chem. A. 2007; 111:12058–12068.(c) Stephens PJ, Devlin FJ, Gasparrini F, Ciogli A, Spinelli D, Cosimelli B. J. Org. Chem. 2007; 72:4707–4715. [PubMed: 17516678] (d) Ding Y, Li X-C, Ferreira D. J. Org. Chem. 2007; 72:9010–9017. [PubMed: 17958369] (e) Berova N, Bari LD, Pescitelli G. Chem. Soc. ReV. 2007; 36:914–931. [PubMed: 17534478] (f) Ding Y; Li X-C, Ferreira D. J. Nat. Prod. 2009; 72:327–335. [PubMed: 19099470]

(9). Yang A, Baker BJ, Grimwade J, Leonard A, McClintock JB. J. Nat. Prod. 1995; 58:1596–1599.

(10). Stuyver LJ, Whitaker T, McBrayer TR, Hernandez-Santiago BI, Lostia S, Tharnish PM, Ramesh M, Chu CK, Jordan R, Shi J, Rachakonda S, Watanabe KA, Otto MJ, Schinazi RF. Antimicrob. Agents Chemother. 2003; 47:244–254. [PubMed: 12499198]

(11). Rao KV, Donia MS, Peng J, Garcia-Palomero E, Alonso D, Martinez A, Medina M, Franzblau SG, Tekwani BL, Khan SI, Wahyuono S, Willett KL, Hamann MT. J. Nat. Prod. 2006; 69:1034–1040. [PubMed: 16872140]

(12). (a) Collins LS, Franzblau SG. Antimicrob. Agents Chemother. 1997; 41:1004–1009. [PubMed: 9145860] (b) Ma G, Khan SI, Jacob MR, Tekwani BL, Li Z, Pasco DS, Walker LA, Khan IA. Antimicrob. Agents Chemother. 2004; 48:4450–4452. NP900281R. [PubMed: 15504880]

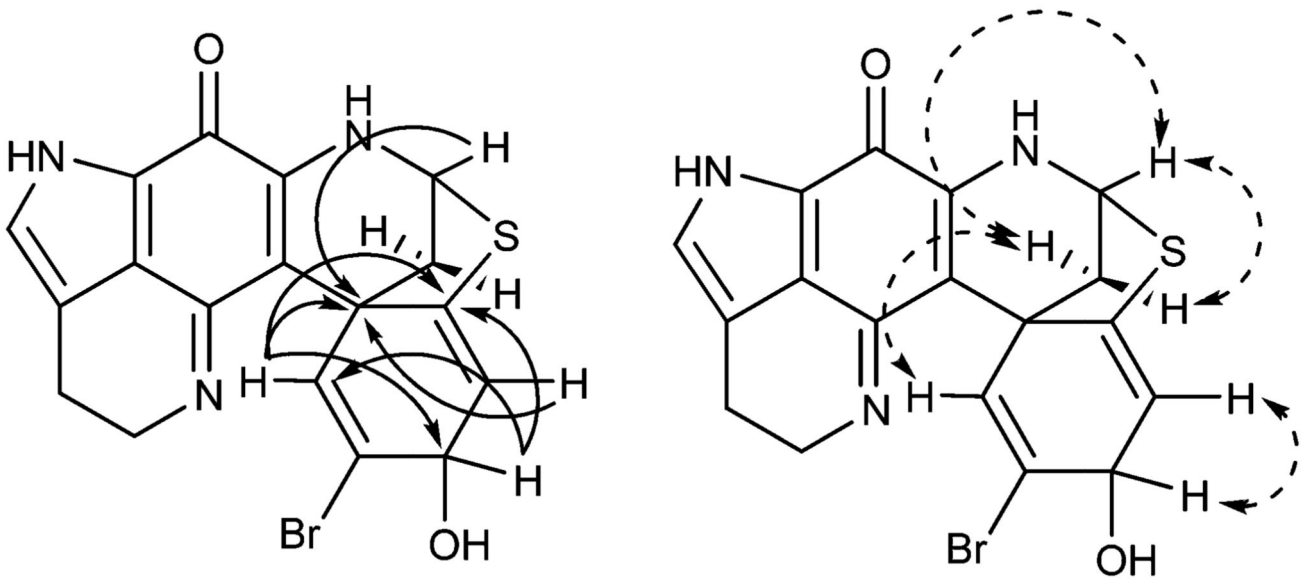

Figure 1.
Key HMBC (→) and NOE (↔) correlations for compound **1**.

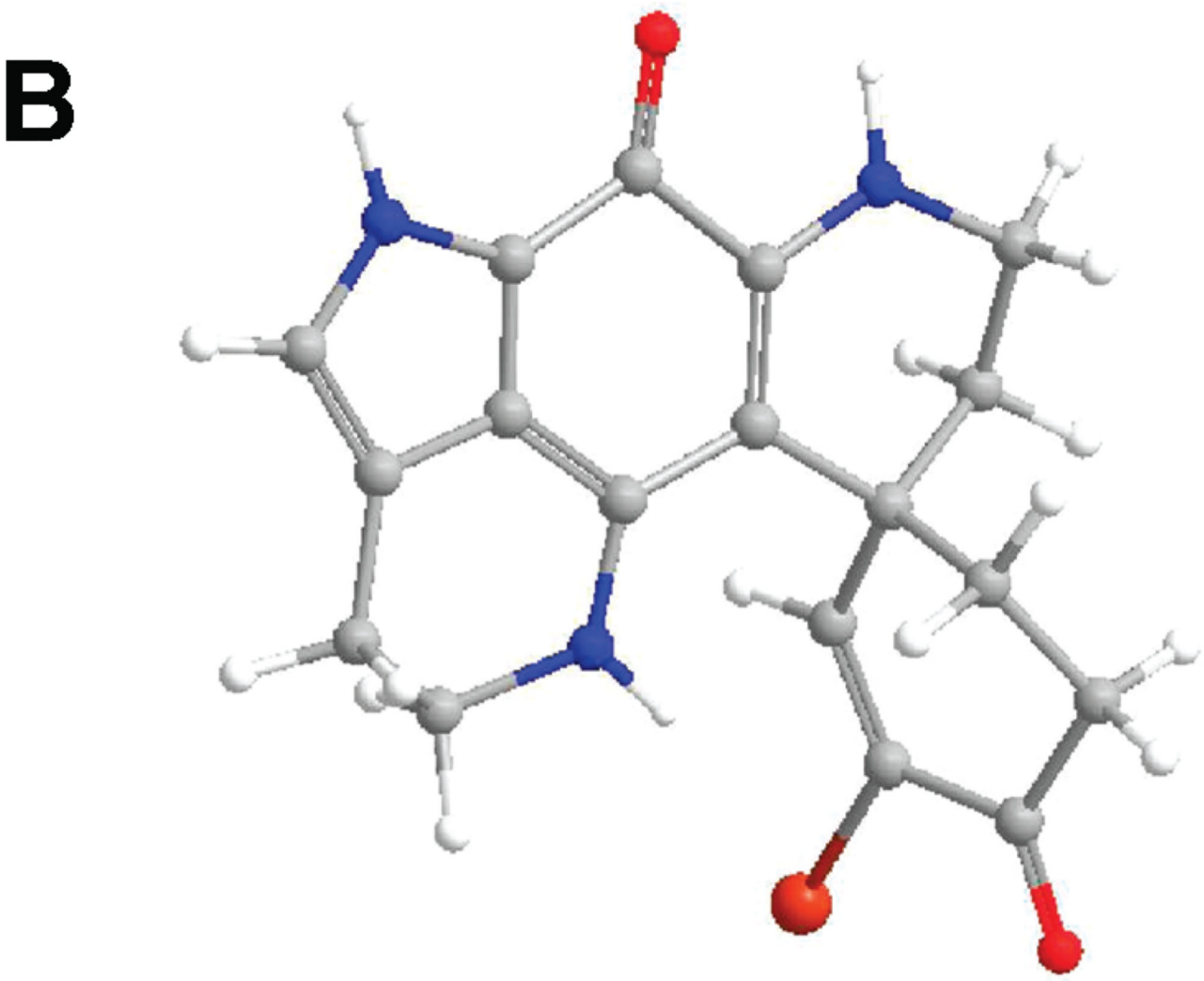

Figure 2.

(A) Calculated and experimental ECD spectra of the formate of discorhabdin Y (**2**) (black line, at the B3LYP/6-31G** level in the gas phase; green line, at the B3LYP/aug-cc-pVDZ// B3LYP/6-31G** level in the gas phase; blue line, experimental in MeOH). (B) Optimized geometry of the discorhabdin Y (**2**) salt at the B3LYP/6-31G** level in the gas phase. (blue, –N; red, –O; dark red, –Br).

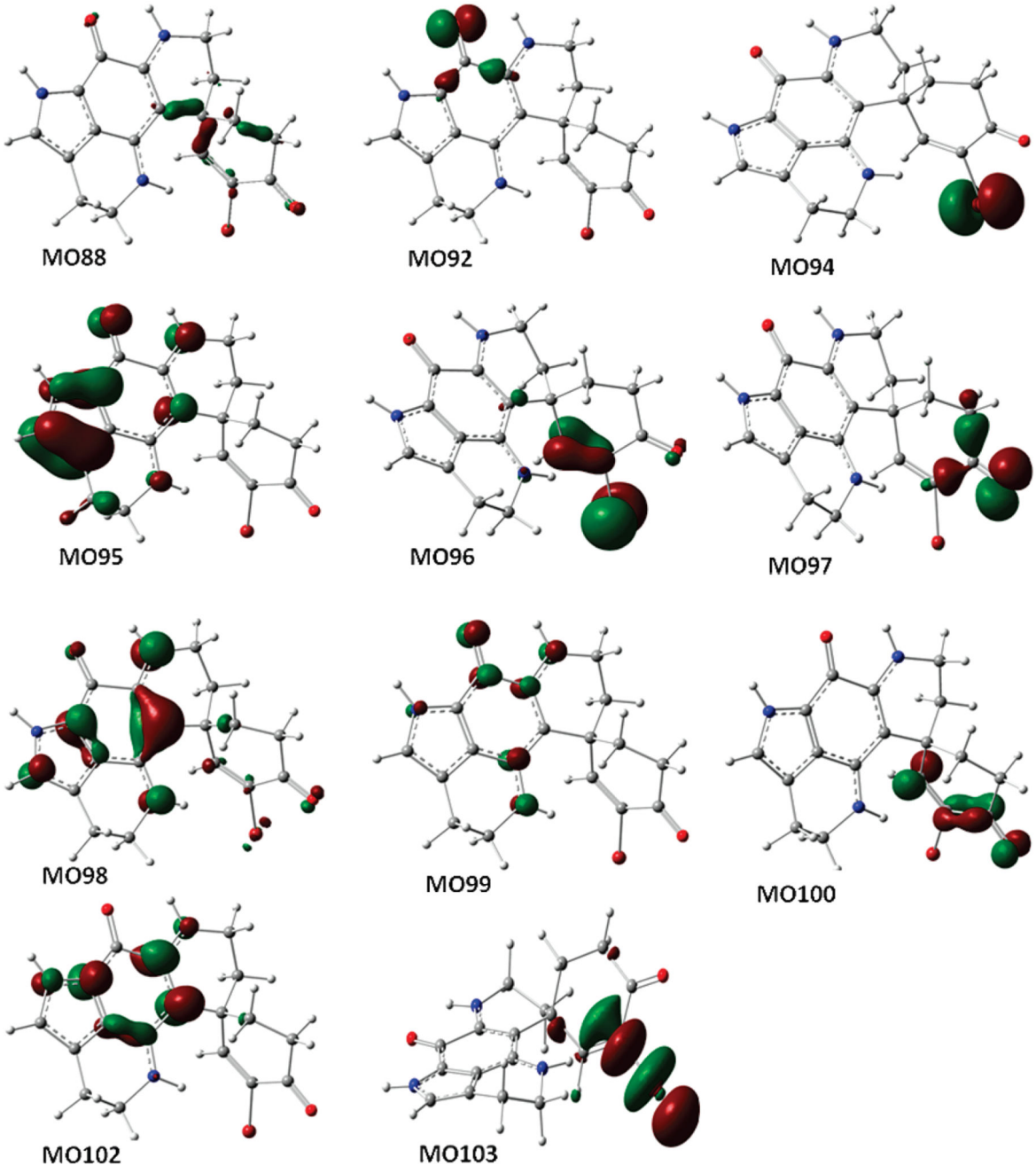

Figure 3.

Some molecular orbitals involved in the key transitions in ECD of the discorhabdin Y (**2**) salt at the B3LYP/6-31G** level in the gas phase.

Table 1

Key Transitions, Oscillator Strengths, and Rotatory Strengths in the ECD Spectrum of Discorhabdin Y (**2**) Salt in the Gas Phase at the B3LYP/6-31G** Level

excited state	ΔE^a (eV)	λ^b (nm)	f^c	$R_{vel}{}^d$	$R_{len}{}^e$
98→99	2.33	531	0.010	16.0	15.7
92→99	3.20	388	0.017	−23.0	−30.0
95→99	3.29	377	0.100	10.9	14.9
94→99	3.34	371	0.013	10.3	11.6
98→100	4.15	299	0.038	−15.3	−17.8
96→100	4.56	272	0.066	−10.3	−12.1
94→100	4.60	270	0.042	13.6	13.0
88→99	5.38	230	0.032	24.2	23.5
96→103	5.96	208	0.021	12.8	14.4
97→102	6.09	204	0.057	−25.0	−26.9

[a] Excitation energy.

[b] Wavelength.

[c] Oscillator strength.

[d] Rotatory strength in velocity form (10^{-40} cgs).

[e] Rotatory strength in length form (10^{-40} cgs).

Table 2

In Vitro Anti-HCV and Antimalarial Activities of Discorhabdins **3**, **4**, and **7**

	anti-HCV activity[a]			antiprotozoal activity[b]			
compound	EC_{90} (μM)	cytotoxicity (Huh-7) at 10 μM	*P. falciparum* (D6 clone) IC_{50} (nM)	SI[c]	*P. falciparum* (W2 clone) IC_{50} (nM)	SI	cytotoxicity (Vero) IC_{50} (μM)
3	<10	cytotoxic	53	130	53	130	6.8
4	<10	cytotoxic	2800	1.0	2000	1.4	2.8
7	<10	cytotoxic	170	58	130	75	9.8

[a] EC_{90}, the 90% effective concentration in the HCV replicon assay; less than 10 μM is considered active.

[b] Assays were run at 4760, 1587, 529, 176, 56, and 19.5 ng/mL and represented as IC_{50}.

[c] SI (selectivity index) = IC_{50} Vero/IC_{50} *P.falciparum*.

Table 3

Antimicrobial Activity of Discorhabdins **3**, **4**, and **7** against AIDS Opportunistic Pathogens and Tuberculosis

	IC_{50} (μM)/MIC (μM)[a]		
compound	**MRSA**	***Mycobacterium intracellulare***	***Mycobacterium tuberculosis* (H37Rv)**
3	4.8/12	0.36/0.74	ND/7.7
4	3.2/11	0.13/0.17	6.8/8.0
7	13/ND	NA	ND/14
ciprofloxacin	1.1/3.0	0.91/1.5	ND
rifampicin	ND	ND	ND/0.21
isoniazid	ND	ND	ND/3.2

[a] IC_{50} is the concentration (μg/mL) that affords 50% inhibition of growth. $IC_{50} \leq 15$ μg/mL is considered active. For compounds that were considered active (≤15 μg/mL), a MIC (minimum inhibitory concentration (μg/mL), lowest tested concentration that allows no detectable growth) was calculated. The screens were run at concentrations of 20, 10, 5, 2.5, 1.25, 0.63, 0.32, 0.16, 0.08, 0.04, and 0.02 μg/mL. NA = not active; ND = not determined.

Table 4

In Vivo Antimalarial Activity of **3**

compound	dose (mg/kg × days)	% parasitemia[a]				
control	10 × 2	11.3	14.0	13.2	12.6	11.4
3	10 × 2	0		6.6	6.9	6.3

[a]Microscopic counts of blood smears prepared from each mouse on day 5 were processed and expressed as percentages of the parasitemia for the individual animals. Mean ± SD (control − (12.5 ± 1.2)) (treated with **3** − (6.6 ± 0.3)).